Symmetries of hadrons after unbreaking the chiral symmetry

L. Ya. Glozman,* C. B. Lang,† and M. Schröck‡
Institut für Physik, FB Theoretische Physik, Universität Graz, A–8010 Graz, Austria
(Dated: March 4, 2013)

We study hadron correlators upon artificial restoration of the spontaneously broken chiral symmetry. In a dynamical lattice simulation we remove the lowest lying eigenmodes of the Dirac operator from the valence quark propagators and study evolution of the hadron masses obtained. All mesons and baryons in our study, except for a pion, survive unbreaking the chiral symmetry and their exponential decay signals become essentially better. From the analysis of the observed spectroscopic patterns we conclude that confinement still persists while the chiral symmetry is restored. All hadrons fall into different chiral multiplets. The broken $U(1)_A$ symmetry does not get restored upon unbreaking the chiral symmetry. We also observe signals of some higher symmetry that includes chiral symmetry as a subgroup. Finally, from comparison of the $\Delta - N$ splitting before and after unbreaking of the chiral symmetry we conclude that both the color-magnetic and the flavor-spin quark-quark interactions are of equal importance.

PACS numbers: 11.15.Ha, 12.38.Gc

I. INTRODUCTION

Highly excited hadrons in the u, d sector reveal some parity doubling [1–10] and possibly some higher symmetry. It was conjectured that this parity doubling reflects effective restoration of chiral symmetry, i.e., insensitivity of the hadron mass generation mechanism to the effects of chiral symmetry breaking in the vacuum [1–6]. Whether this conjecture is correct or not can be answered experimentally since the conjectured symmetry requires existence of some not yet observed states.

Recent and most complete experimental analysis on highly excited nucleons that includes not only elastic πN, but also the photoproduction data, does report evidence for some of the missing states and the parity doubling patterns look now even better than before [11].

The question of a possible symmetry in hadron spectra is one of the central questions for QCD since it would help to understand dynamics of confinement and chiral symmetry breaking as well as their role for the hadron mass generation.

Another "experimental" tool to address the issue of the hadron mass generation is lattice QCD. Equipped with the QCD Lagrangian and Monte-Carlo techniques, one can calculate, at least in principle, hadron masses and other hadron properties from first principles. Enormous progress has been achieved for the hadron ground states. The problem of excited states, especially above the multihadron thresholds like πN, $\Delta\pi$, $\pi\pi$, $\pi\rho$, ... turns out to be much more difficult and demanding than was initially anticipated. When it is solved lattice results should reproduce experimental patterns and possibly indicate some still missing states.

Still, the mass of a hadron by itself, obtained from the experiment or from the lattice simulations, tells us not so much about the physics which is behind the mass generation. The pattern of all hadrons, on the contrary, could shed some light on the underlying dynamics if there are some obvious symmetries in the pattern or if its regularities can be systematically explained.

The most interesting issue is to get some insight on how QCD "works" in some important cases and understand the underlying physical picture. In this sense one can use lattice QCD as a tool to explore the interrelations between confinement and chiral symmetry breaking. In particular, we can ask the question whether hadrons and confinement will survive after having artificially removed the quark condensate of the vacuum. This can be achieved via removal of the low-lying eigenmodes of the Dirac operator, which is a well defined procedure [12, 13].

In the past mainly the opposite was explored. After suggestions within the instanton liquid model [14] the effect of the low-lying chiral modes on the ρ and other correlators was studied on the lattice. In a series of papers [12, 15–17] it was shown that low modes saturate the pseudoscalar and axial vector correlators at large distances and do not affect the part where high-lying states appear. In [12, 18] low mode saturation and also effects of low mode removal for mesons were studied for quenched configurations with the overlap Dirac operator [19, 20]. Subsequently low modes were utilized to improve the convergence of the determination of hadron propagators [12, 18, 21–24] studying the efficiency when using the low modes of the Dirac operator or the Hermitian Dirac operator.

We are studying the complementary case, i.e., removal of the low modes and we will refer to this as "unbreaking" the chiral symmetry. This issue has been addressed in a recent paper [25, 26] where the low-lying eigenmodes of the Dirac operator have been removed from the quark Green's function and masses of the lowest mesons π, ρ, a_0

* leonid.glozman@uni-graz.at
† christian.lang@uni-graz.at
‡ mario.schroeck@uni-graz.at

and a_1 have been calculated with such truncated quark propagators. The truncated Landau gauge quark propagator itself has been investigated in [27] where the loss of dynamical mass generation in the infrared sector of the propagator has been demonstrated.

After the unbreaking of the chiral symmetry the signal from the π-meson, obtained with the pseudoscalar quark-antiquark operator, disappears, which is consistent with the (pseudo) Goldstone boson nature of the pion. Indeed, with the artificially restored chiral symmetry there cannot be Goldstone bosons. What is very interesting, is that other low-lying mesons survive and the quality of their signals become even essentially better after extraction of the low-lying eigenmodes of the Dirac operator, responsible for chiral symmetry breaking. The very fact that hadrons survive the unbreaking of the chiral symmetry tells that there is confinement in the system even without the quark condensate. (A similar behavior was found in [28, 29], where the effect of such a removal on the static quark potential was studied.)

After extraction of the quark condensate the lowest-lying ρ and a_1 mesons demonstrate restoration of the chiral symmetry - they become degenerate - and their mass is rather large. This disproves a rather popular assertion that, e.g., the ρ-mass is entirely due to the quark condensate of the vacuum. As a physical implication we should then not expect a drop off the ρ-mass in a dense medium, which is a very popular issue both theoretically and experimentally for the last two decades [30]. This result should also be of importance for a debated issue of confining but chirally symmetric matter at low temperatures and large density [31–34].

The conclusion of [25] about survival of confinement after unbreaking of the chiral symmetry was obtained on the limited basis of the lowest-lying mesons. In order to see it more clearly we need to extend the number of extracted states, in particular to include radially and orbitally excited hadrons (following quark model terminology). Consequently, we now add the b_1 and ρ' states to the above mentioned list of mesons. We limit ourselves only to the isovector mesons since the isoscalar mesons would require inclusion of disconnected graphs, which is numerically very costly.

Most importantly, we study behavior of the ground and excited positive and negative parity states in the N and Δ spectra. The baryonic states add additional information about existence or nonexistence of confinement. They do allow to see that confinement does survive after the restoration of chiral symmetry. Second, we see some traces of the higher symmetry, higher than simply $SU(2)_R \times SU(2)_L$. This observation may be related with the higher symmetry seen in the highly excited hadrons.

Our paper is organized as follows. In the next section we remind on the connection between low eigenmodes of the Dirac operator and the quark condensate in the vacuum. We discuss some basic aspects of removal of Dirac eigenmodes from the quark propagator. In Sect. III we present the details of the lattice simulation. The fourth section is devoted to the description of the baryon and meson interpolators used for our study of hadrons. In Sect. V we show and analyze the results and draw conclusions. Finally, in the last section, we briefly summarize our main observations.

II. THE QUARK CONDENSATE AND THE DIRAC OPERATOR

The lowest eigenmodes of the Dirac operator are related (in the chiral limit) to the quark condensate of the vacuum. This is encoded in the Banks–Casher relation [35]

$$< 0|\bar{q}q|0 >= -\pi\rho(0) \ , \tag{1}$$

where $\rho(0)$ is a density of the lowest quasi-zero eigenmodes of the Dirac operator. Here the sequence of limits is important: first, the infinite volume limit at finite quark mass is assumed and then the chiral limit should be taken. The opposite sequence would produce no chiral condensate as in the finite volume there cannot be any spontaneous breaking of chiral symmetry.

All lattice calculations are performed on a lattice of a finite volume. In the finite lattice volume the spectrum of the Dirac operator is discrete and the energy of the lowest nonzero mode of the Dirac operator is finite. Consequently, the quark condensate is strictly speaking zero. However, increasing the lattice volume the gap in the spectrum of the eigenmodes becomes smaller and smaller and the density of the lowest nonzero eigenmodes increases. A well defined limit of this density scaling exists: the number of such eigenvalues in a given interval adjacent to the real axis scales with the lattice volume. (In [36] is is argued[1] that the number of relevant eigenvalues should scale proportional the square root of the number of lattice points.)

In [24, 25] it was established that the eigenmodes of the Hermitian Dirac operator $D_5 \equiv \gamma_5 D$ result in a faster saturation of the pseudoscalar correlator when approximating quark propagators by the lowest eigenmodes only, compared to the eigenmodes of the Dirac operator D. Therefore, we focus on reducing the quark propagators in terms of eigenmodes of D_5 rather than D.

From the lattice calculations in a given finite volume we cannot say a priori which and how many lowest eigenmodes of the Dirac operator are responsible for the quark condensate of the vacuum. For the overlap operator the real eigenvalues correspond to exact chiral modes, the zero modes (instantons); for Wilson-type operators one may associate real eigenvalues with zero modes. Their weight is suppressed in the infinite volume limit. The Banks-Casher relation, however, relies only on the density of nonzero modes. For the Hermitian Dirac operator

[1] We thank Kim Splittorff for pointing us to that reference

D_5 there is no simple method to distinguish between the real modes of the D and its small, but complex modes. In [25, 26] we discuss the integral over the distribution of the (real) eigenvalues of D_5. There we observe a transition region up to roughly twice the size of the quark mass corresponding to $\mathcal{O}(16-32)$ eigenmodes, as also observed in, e.g., [37–40].

We follow the procedure to remove an increasing number of the lowest Dirac modes and study the effects of the (remaining) chiral symmetry breaking on the masses of hadrons. To be specific, we construct reduced quark propagators

$$S_{\mathrm{red}(k)} = S - S_{\mathrm{lm}(k)} \equiv S - \sum_{i \le k} \mu_i^{-1} |v_i\rangle\langle v_i|\gamma_5 \ , \qquad (2)$$

where S is the standard quark propagator obtained from the inversion of the Dirac operator, the μ_i are the (real) eigenvalues of D_5, $|v_i\rangle$ are the corresponding eigenvectors and k represents the reduction parameter which will be varied from $0-128$.

Note that the low-mode contribution (lm) of the quark propagators, $S_{\mathrm{lm}(k)}$, must act on the same quark sources as S, see discussion below.

III. THE SETUP

A. Dirac operator

For the dynamical quarks of our configurations as well as for the valence quarks of our study the so called chirally improved (CI) Dirac operator [41, 42] has been used. The latter represents an approximate solution to the Ginsparg–Wilson equation and therefore offers better chiral properties than the Wilson Dirac operator while being less expensive, in terms of computation time, in comparison to the chirally exact overlap operator.

B. Gauge configurations

We performed our study on 161 gauge field configurations [43, 44] that were generated for two degenerate dynamical light CI fermions with a corresponding pion mass $m_\pi = 322(5)\,\mathrm{MeV}$. The lattice size is $16^3 \times 32$ and the lattice spacing $a = 0.144(1)\,\mathrm{fm}$.

C. Quark source smearing

In order to obtain quark propagators, the Dirac operator has to be inverted on given quark sources. To improve the signal in hadron correlators, extended sources of Gaussian form [45, 46] instead of point sources are being used. Using several different extended sources allows for a larger operator basis in the variational method [47–49]. We use three different kinds of sources: narrow ($0.27\,\mathrm{fm}$) and wide ($0.55\,\mathrm{fm}$) sources, which are approximately of Gaussian shape, and a derivative source.

The narrow (wide) sources will be denoted by a subscript n (w) of the quark fields and the derivative source by ∂_i, respectively. The details of the calculation of the smeared quark sources are given in [44].

D. Variational method

In order to disentangle the excited states from the ground state (and also to provide cleaner signals for the ground states) we use the variational method [47, 48]. One computes cross-correlators $C_{ik}(t) = \langle O_i(t) O_k(0)^\dagger \rangle$ between several different lattice interpolators and solves the generalized eigenvalue problem

$$C(t)\vec{u}_n(t) = \lambda_n(t) C(t_0) \vec{u}_n(t) \ , \qquad (3)$$

in order to approximately recover the energy eigenstates $|n\rangle$. The eigenvalues allow us to get the energy values $\lambda_n(t) \sim \exp(-E_n\, t)$ and the eigenvectors serve as fingerprints of the states, indicating their content in terms of the lattice interpolators. In our plots we show $\lambda_n(t)$, the effective masses $E_n(t) = \log(\lambda_n(t)/\lambda_n(t+1))$ and the t-dependence of the eigenvectors in order to verify the state identification. The quality of the results depends on the statistics and the provided set of lattice operators (for a discussion see [44]). The used interpolators are discussed in Sect. IV.

E. Dirac eigenmodes

On the given gauge field configurations we calculated the lowest 128 eigenmodes of the Hermitian Dirac operator D_5 using ARPACK which is an implementation of the Arnoldi method to calculate a part of the spectrum of arbitrary matrices [50].

Once the eigenmodes have been calculated and the quark propagators S have been obtained by inverting the Dirac operator on the three types of sources mentioned in Sec. III C, we can construct the reduced propagators $S_{\mathrm{red}(k)}$ according to (2) after multiplying the low-mode part of the propagator, $S_{\mathrm{lm}(k)}$, with the same three source types, respectively.

IV. HADRON INTERPOLATORS

Here we list the baryons and mesons we studied under Dirac low-mode reduction and give the interpolating fields for each individual.

A. Baryons

We analyze the nucleon and Δ baryons both with positive and negative parity. For the interpolators we use

$\chi^{(i)}$	$\Gamma_1^{(i)}$	$\Gamma_2^{(i)}$	smearing	$\#_N$
$\chi^{(1)}$	$\mathbb{1}$	$C\,\gamma_5$	$(nn)n$	1
			$(nn)w$	2
			$(nw)n$	3
			$(nw)w$	4
			$(ww)n$	5
			$(ww)w$	6
$\chi^{(2)}$	γ_5	C	$(nn)n$	7
			$(nn)w$	8
			$(nw)n$	9
			$(nw)w$	10
			$(ww)n$	11
			$(ww)w$	12
$\chi^{(3)}$	$i\,\mathbb{1}$	$C\,\gamma_t\,\gamma_5$	$(nn)n$	13
			$(nn)w$	14
			$(nw)n$	15
			$(nw)w$	16
			$(ww)n$	17
			$(ww)w$	18

TABLE I. Interpolators for the N channel. The Dirac structures $\chi^{(i)}$, the quark smearings and the corresponding interpolator numbers $\#_N$ are given.

Gaussian smeared quark sources (n and w). For the nucleon we adopt three different Dirac structures, resulting in 18 interpolators (see Tab. I) where we left out those operators that are similar to other ones due to isospin symmetry. The construction of the nucleon interpolators is given by

$$N^{(i)} = \epsilon_{abc}\,\Gamma_1^{(i)}\,u_a\left(u_b^T\,\Gamma_2^{(i)}\,d_c - d_b^T\,\Gamma_2^{(i)}\,u_c\right). \qquad (4)$$

For the Δ,

$$\Delta_k = \epsilon_{abc}\,u_a\left(u_b^T\,C\,\gamma_k\,u_c\right), \qquad (5)$$

we use only one Dirac structure and the six corresponding interpolators are listed in Tab. II. We use parity projection for all baryons and Rarita-Schwinger projection for the Δ [44]. The sink interpolators are also projected to zero spatial momentum.

B. Mesons

We investigate isovector mesons of spin 1. Isoscalars require the calculation of disconnected graphs which are computationally too demanding for the type of fermion action used. The scalar meson a_0 as well as the pseudoscalar pion was studied already in [25].

Thus, the studied nonexotic channels are the J^{PC} combinations 1^{--} (ρ), 1^{++} (a_1) and 1^{+-} (b_1). For the analysis of the mesons we include derivative sources [51] in the construction of the interpolators to provide a large

smearing	$\#_\Delta$
$(nn)n$	1
$(nn)w$	2
$(nw)n$	3
$(nw)w$	4
$(ww)n$	5
$(ww)w$	6

TABLE II. Interpolators for the Δ channel. The quark smearings and the corresponding interpolator numbers $\#_\Delta$ are given.

$\#_\rho$	interpolator(s)
1	$\overline{a}_n\gamma_k b_n$
8	$\overline{a}_w\gamma_k\gamma_t b_w$
12	$\overline{a}_{\partial_k} b_w - \overline{a}_w b_{\partial_k}$
17	$\overline{a}_{\partial_i}\gamma_k b_{\partial_i}$
22	$\overline{a}_{\partial_k}\epsilon_{ijk}\gamma_j\gamma_5 b_w - \overline{a}_w\epsilon_{ijk}\gamma_j\gamma_5 b_{\partial_k}$
$\#_{a_1}$	interpolator(s)
1	$\overline{a}_n\gamma_k\gamma_5 b_n$
2	$\overline{a}_n\gamma_k\gamma_5 b_w + \overline{a}_w\gamma_k\gamma_5 b_n$
4	$\overline{a}_w\gamma_k\gamma_5 b_w$
$\#_{b_1}$	interpolator(s)
6	$\overline{a}_{\partial_k}\gamma_5 b_n - \overline{a}_n\gamma_5 b_{\partial_k}$
8	$\overline{a}_{\partial_k}\gamma_5 b_w - \overline{a}_w\gamma_5 b_{\partial_k}$

TABLE III. Interpolators for (top) the ρ-meson, $J^{PC} = 1^{--}$, (middle) the a_1-meson, $J^{PC} = 1^{++}$, and (bottom) the b_1-meson, $J^{PC} = 1^{+-}$. The first column shows the number, the second shows the explicit form of the interpolator. The numbers refer to the classification in [52].

operator basis for the variational method. In Table III we list only those interpolators explicitly whose combination resulted in a good signal in practice when plugged into the variational method. The sink interpolators are projected to zero spatial momentum. A more complete list of possible interpolating fields is given in [44, 52].

V. RESULTS AND DISCUSSION

A. Truncation study

The reduction parameter k in (2) gives the number of the lowest eigenmodes of the Dirac operator removed from the quark propagator. We study reduced quark propagators with $k = 0, 2, 4, 8, 12, 16, 20, 32, 64, 128$ and three different quark smearings (n, w, ∂_i). These are then combined into different hadron propagators and the correlation matrix for a hadron with given quantum numbers is calculated. The variational method is used to extract the ground and excited states of that hadron. Con-

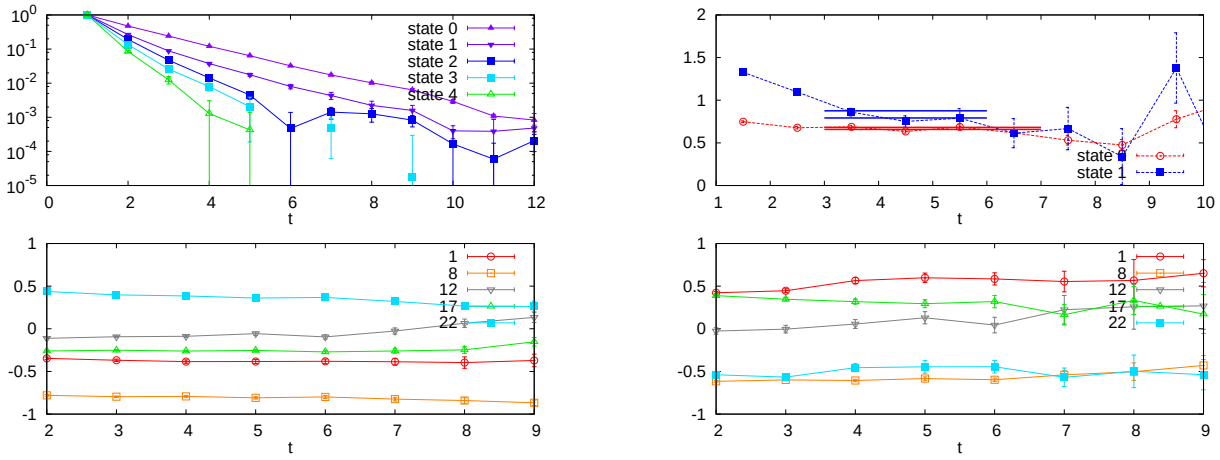

FIG. 1. ρ with 12 eigenmodes subtracted: The correlators for all eigenstates (upper left), effective mass plot for the two lowest states (upper right), eigenvectors corresponding to the ground state (lower left). and 1st excited state (lower right).

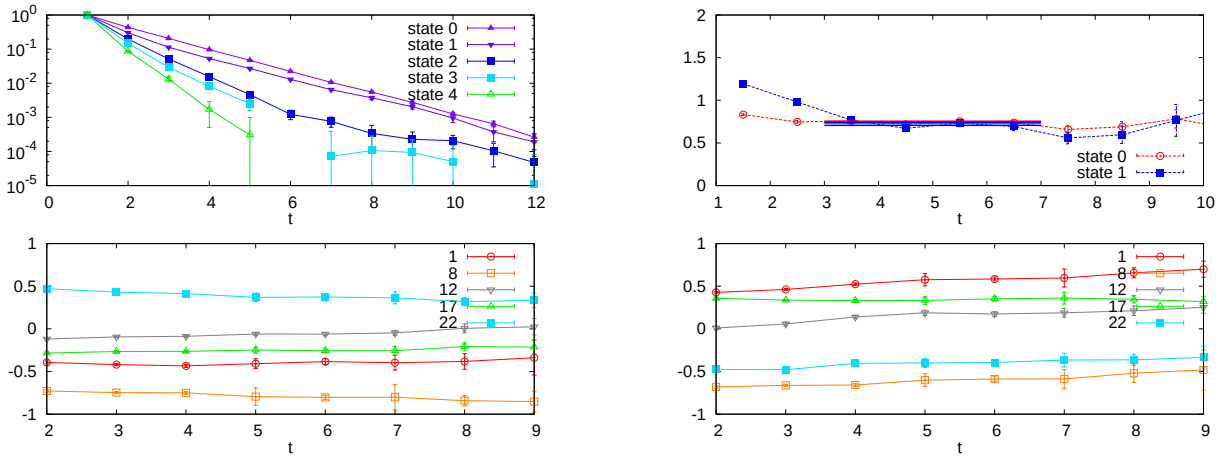

FIG. 2. ρ with 32 eigenmodes subtracted: The correlators for all eigenstates (upper left), effective mass plot for the two lowest states (upper right), eigenvectors corresponding to the ground state (lower left). and 1st excited state (lower right).

sequently, we observe and study the evolution of hadron masses as a function of the number of the subtracted lowest eigenmodes. Increasing the number of the subtracted lowest eigenmodes we gradually remove the chiral condensate of the vacuum and consequently "unbreak" the chiral symmetry.

Typical results for the mesons and baryons under study are shown in Figs. 1 - 12. For each hadron we show in the figures two representative reduction levels k for which we also show explicitly all eigenvalues stemming from the variational method, i.e., the correlators corresponding to different energy levels. Moreover, we show for the ground and first excited state (where applicable) the eigenvector components and the effective mass plots including fit ranges and values. The energy values are determined from exponential fits to the eigenvalues over the indicated fit ranges.

In Figs. 1 and 2 we show the eigenvalues and eigenvectors (cf. Sect. III D) and the effective mass plots for the ground and excited states of the ρ-meson ($J^{PC} = 1^{--}$) after having subtracted 12 and 32 eigenmodes of D_5. (The results for the untruncated situation, with higher statistics and for several more parameter sets are shown in [52].) The eigenvector composition for both states is stable and clearly distinct. The mass splitting between ground state and excited state disappears with increasing truncation level.

For the meson channels a_1 and b_1 the statistics allow only to determine the ground state in a reliable way. In the case of the a_1 ($J^{PC} = 1^{++}$) meson (Fig. 3 for $k = 4$ and $k = 64$) and for the b_1 ($J^{PC} = 1^{+-}$) meson (Fig. 4 for $k = 2$ and $k = 128$) we thus show only the ground states. We observe improved plateau quality for the effective masses when increasing number of truncated modes.

In Fig. 5 the nucleon of positive parity (the ground state and its first excitation, $J^P = \frac{1}{2}^+$), after having subtracted the lowest 20 eigenmodes is shown. These should be compared with Fig. 6 where 64 modes have

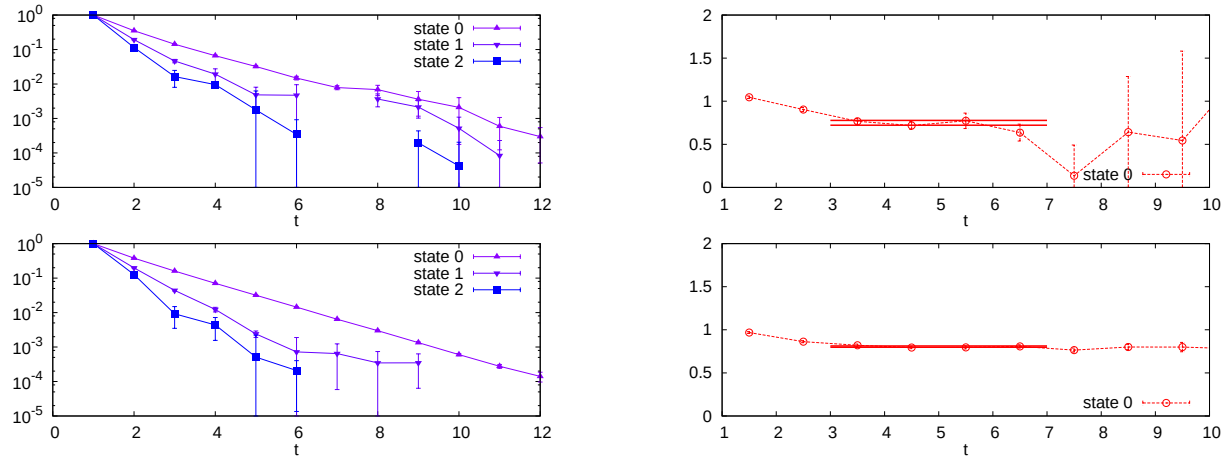

FIG. 3. a_1 with 4 (upper row) and 64 (lower row) eigenmodes subtracted: The correlators for all eigenstates (left), effective mass plot for the lowest state (right).

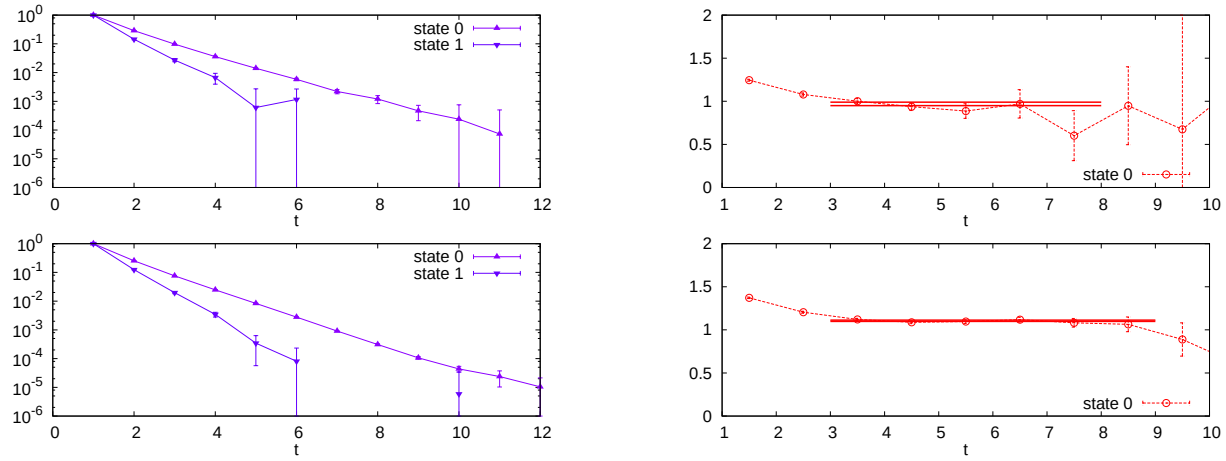

FIG. 4. b_1 with 2 (upper row) and 128 (lower row) eigenmodes subtracted: The correlators for all eigenstates (left), effective mass plot for the lowest state (right).

been subtracted. In Fig. 7 and 8 we present two nucleon states of negative parity, $J^P = \frac{1}{2}^-$, (at reduction level 12 and 64).

The positive parity Δ ground and excited states, $J^P = \frac{3}{2}^+$ at reduction level 16 and 128 are shown in Fig. 9 and Fig. 10 and the negative parity Δ's ($J^P = \frac{3}{2}^-$) at the same reduction levels are given in Fig. 11 and Fig. 12, respectively.

An obvious observation is that the quality of the signal (the quality of plateaus) essentially improves with increasing the number of removed eigenmodes for all hadrons under study. This fact makes it easier to reliably identify masses of states after unbreaking the chiral symmetry. In many cases for excited hadrons the quality of plateaus before unbreaking of the chiral symmetry is rather poor, but after removing more and more eigenmodes of the Dirac operator it becomes better and better, so eventually it allows to unambiguously establish that indeed we see the state, even though with the untruncated propagators the identification of the state would be less clear.

A plausible explanation for this phenomenon would be that by unbreaking the chiral symmetry we remove from the hadron its pion cloud and subtract all higher Fock components like πN, $\pi\Delta$, $\pi\pi$, and so on from the hadron wave functions. It is these components related to the chiral symmetry breaking that couple excited and not excited hadrons to each other and render signals from the excited states poor in fully untruncated QCD.

B. Confinement after unbreaking the chiral symmetry

The most interesting question is whether hadrons and confinement survive the unbreaking of the chiral symmetry. To discuss this issue we put all the results from the previous figures together and analyze how masses of

the considered hadrons change with the reduction level. Therefore, the relevant truncation scale is not the Dirac operator eigenmode index k itself, since it has to scale with the lattice volume when keeping the physics constant. Instead, we introduce a cutoff parameter σ such that the reduction level σ means that all μ_k for which $|\mu_k| < \sigma$ have been excluded in the underlying quark propagators [25]. We still give the corresponding index k on the upper horizontal scale of the plots.

The masses of all studied hadrons under D_5 eigenmode reduction are summarized in Fig. 13. The scale is set by the Sommer parameter (i.e., by the static potential acting between two heavy quarks, in other words, by the gluonic dynamics). The physics of the static potential knows nothing about the valence quarks and the truncation of lowest lying eigenmodes of the Dirac operator for the light valence quarks. It implies that these plots suggest at least qualitatively the evolution of the hadron masses in absolute units of energy. We observe approximately a universal growth of all hadron masses with equal slope after subtraction of a sufficient amount of the chiral modes of the Dirac operator. In this regime chiral symmetry is approximately restored and the whole hadron mass is not related to chiral symmetry breaking. A universal slope might be interpreted as an indication to a universal growth of the hadron size.

Assume that after having unbroken the chiral symmetry the exponential decay signals from all hadrons would disappear. This would indicate that with the artificial restoration of the chiral symmetry confinement also vanishes and that there is a direct connection between the confinement in QCD and the lowest lying modes of the Dirac operator. Contrary to that we observe a very clear signal from all hadrons, except for a pion. This suggests that confinement survives the unbreaking of the chiral symmetry.

However, there is still the possibility that this clear signal comes from the unconfined (unbound) quarks with some mass m_0 at a given truncation level. In this case we would expect at a given truncation level a universal scaling law with all mesons having the mass $2\,m_0$ and all baryons with the mass $3\,m_0$. There would be no excited states of hadrons.

In order to address this issue we show in Fig. 14 all hadron masses in units of the ρ-meson mass obtained at the same truncation level. Indeed, some of the states – such as a_1 and ρ', as well as the ground and the first excited states of the nucleon of both parities – do follow this behavior of mass $2\,m_0$ and $3\,m_0$ for mesons and baryons, respectively. However, this is definitely not the case for the b_1 state as well as for the Δ-resonance and especially its first excited states of positive and negative parity. Given that the signal in all latter cases is unambiguous, we conclude that there is no universal scaling ($2\,m_0$ for mesons and $3\,m_0$ for baryons) for all hadrons. This rules out the possibility that our signals are produced by the unbound (unconfined) quarks. We do observe confined hadrons.

Actually, this can be seen also from another perspective. The mass m_0 is large and increases with truncation of the quark propagators. At the same time we observe chiral restoration in the correlators (e.g., a_1 and ρ). The large mass m_0 of unconfined free quarks then contradicts restoration of chiral symmetry. This supports our argument that we do not observe unconfined quarks.

The fact that masses of some of the mesons and some of the baryons get degenerate and are related through a simple law $2\,m_0$ for mesons and $3\,m_0$ for baryons indicates symmetries of hadrons that appear after unbreaking (restoration) of the chiral symmetry.

C. Meson degeneracies and splittings and what they tell us

Restoration of the $SU(2)_L \times SU(2)_R$ chiral symmetry in the vacuum requires the states to fall into parity-chiral multiplets [2–6]. Below we shortly summarize a content of these parity-chiral multiplets for the mesons in our study.

The full set of multiplets of the parity-chiral group $SU(2)_L \times SU(2)_R \times C_i$, where the group C_i consists of identity and the space inversion, for the $J = 1$ mesons is as follows:

$$
\begin{array}{lcll}
(0,0) & : & \omega(0,1^{--}) & f_1(0,1^{++}) \\
(\frac{1}{2},\frac{1}{2})_a & : & h_1(0,1^{+-}) & \rho(1,1^{--}) \\
(\frac{1}{2},\frac{1}{2})_b & : & \omega(0,1^{--}) & b_1(1,1^{+-}) \\
(0,1)+(1,0) & : & a_1(1,1^{++}) & \rho(1,1^{--})
\end{array}
$$

Note, that the unbroken chiral $SU(2)_L \times SU(2)_R$ symmetry requires existence of two independent ρ-mesons, one of them is the chiral partner of the h_1 meson, and the other one of the a_1 state. Similar is true for the ω-meson.

The states from two distinct multiplets $(\frac{1}{2},\frac{1}{2})_a$ and $(\frac{1}{2},\frac{1}{2})_b$ that have the same isospin but opposite spatial parity are connected to each other by the $U(1)_A$ transformation, if the $U(1)_A$ symmetry is broken neither explicitly nor spontaneously. In our real world $U(1)_A$ is broken both explicitly via the axial anomaly and spontaneously via the quark condensate of the vacuum. So in the world with restored $U(1)_A$ symmetry a ρ meson, that is the chiral partner to the h_1 meson, would be degenerate with the b_1 state. The h_1, ρ, ω and b_1 states would form an irreducible multiplet of the $SU(2)_L \times SU(2)_R \times U(1)_A$ group.

On top of the chirally symmetric vacuum the $\rho - a_1$ splitting vanishes, see, e.g., Figs. 13 and 14., a clear signal of the chiral $SU(2)_L \times SU(2)_R$ symmetry restoration in the physical states. At the same time large $b_1 - \rho$ and $b_1 - \rho'$ splittings persist. This is a direct indication that the $U(1)_A$ breaking does not disappear. While that $U(1)_A$ breaking component that is due to the chiral condensate should vanish with the condensate, the $U(1)_A$

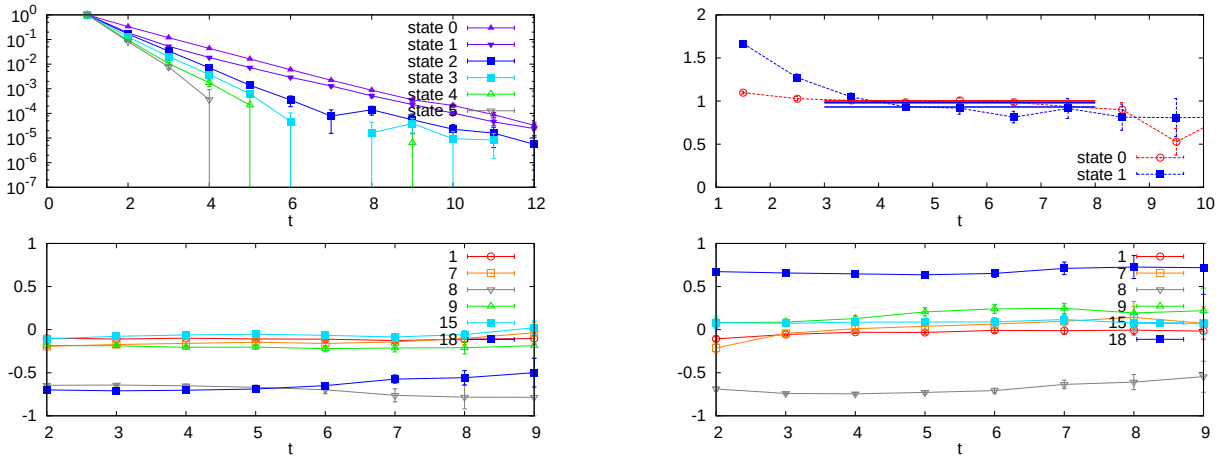

FIG. 5. $N(+)$ with 20 eigenmodes subtracted: The correlators for all eigenstates (upper left), effective mass plot for the two lowest states (upper right), eigenvectors corresponding to the ground state (lower left). and 1st excited state (lower right).

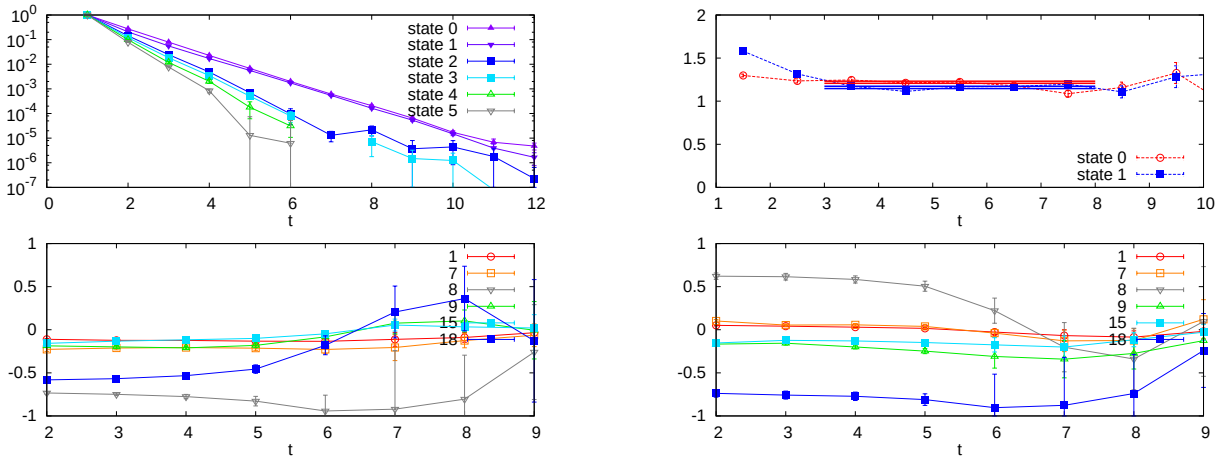

FIG. 6. $N(+)$ with 64 eigenmodes subtracted: The correlators for all eigenstates (upper left), effective mass plot for the two lowest states (upper right), eigenvectors corresponding to the ground state (lower left). and 1st excited state (lower right).

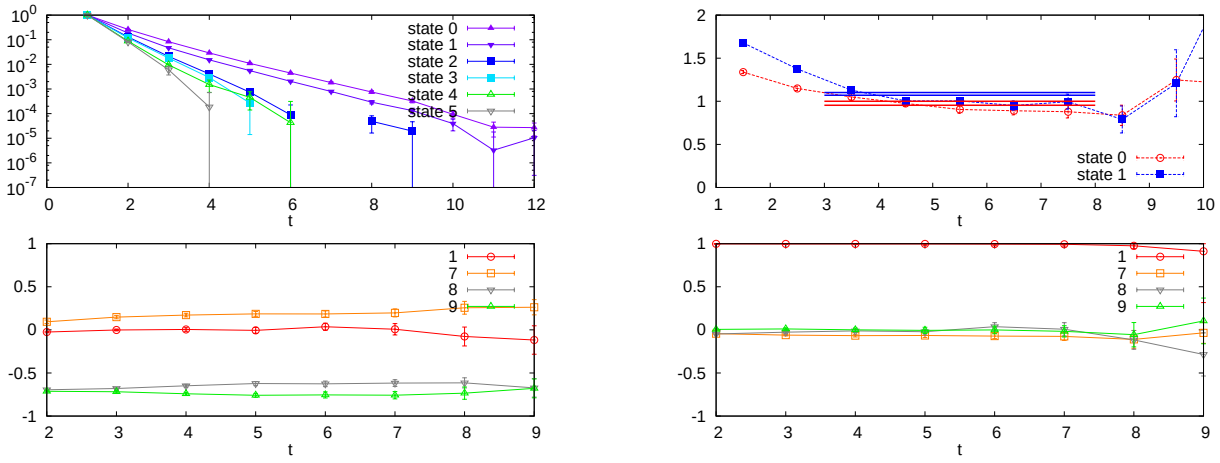

FIG. 7. $N(-)$ with 12 eigenmodes subtracted: The correlators for all eigenstates (upper left), effective mass plot for the two lowest states (upper right), eigenvectors corresponding to the ground state (lower left). and 1st excited state (lower right).

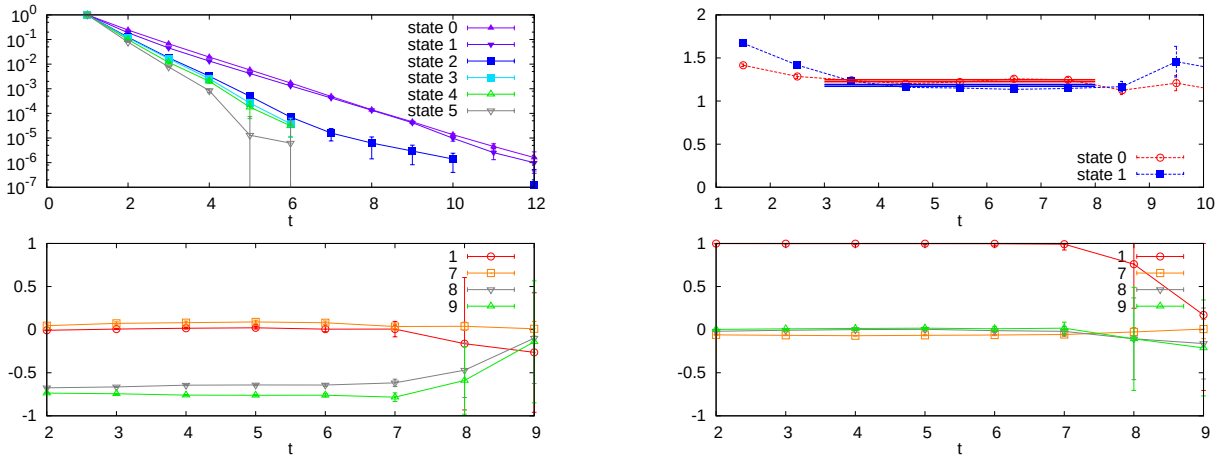

FIG. 8. $N(-)$ with 64 eigenmodes subtracted: The correlators for all eigenstates (upper left), effective mass plot for the two lowest states (upper right), eigenvectors corresponding to the ground state (lower left). and 1st excited state (lower right).

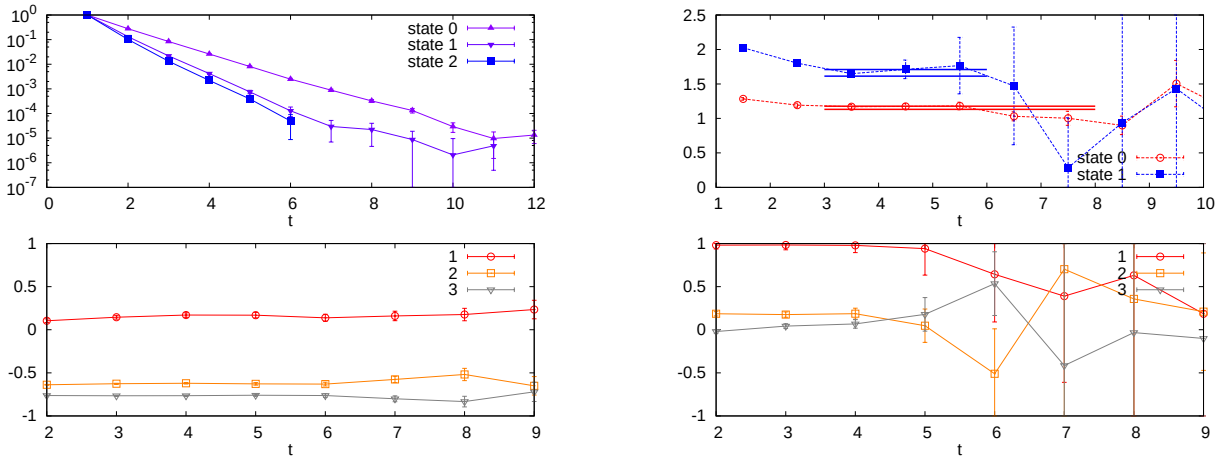

FIG. 9. $\Delta(+)$ with 16 eigenmodes subtracted: The correlators for all eigenstates (upper left), effective mass plot for the two lowest states (upper right), eigenvectors corresponding to the ground state (lower left). and 1st excited state (lower right).

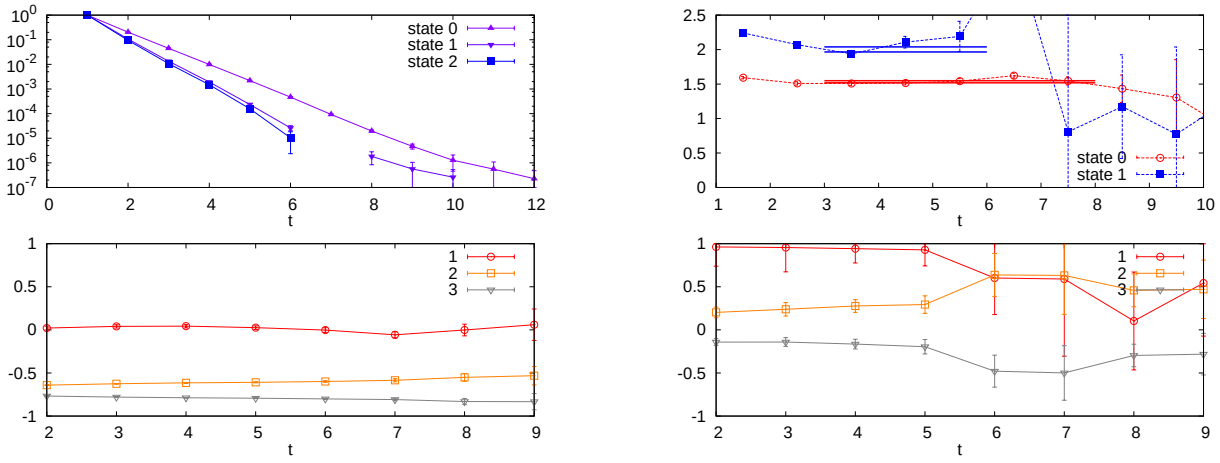

FIG. 10. $\Delta(+)$ with 128 eigenmodes subtracted: The correlators for all eigenstates (upper left), effective mass plot for the two lowest states (upper right), eigenvectors corresponding to the ground state (lower left). and 1st excited state (lower right).

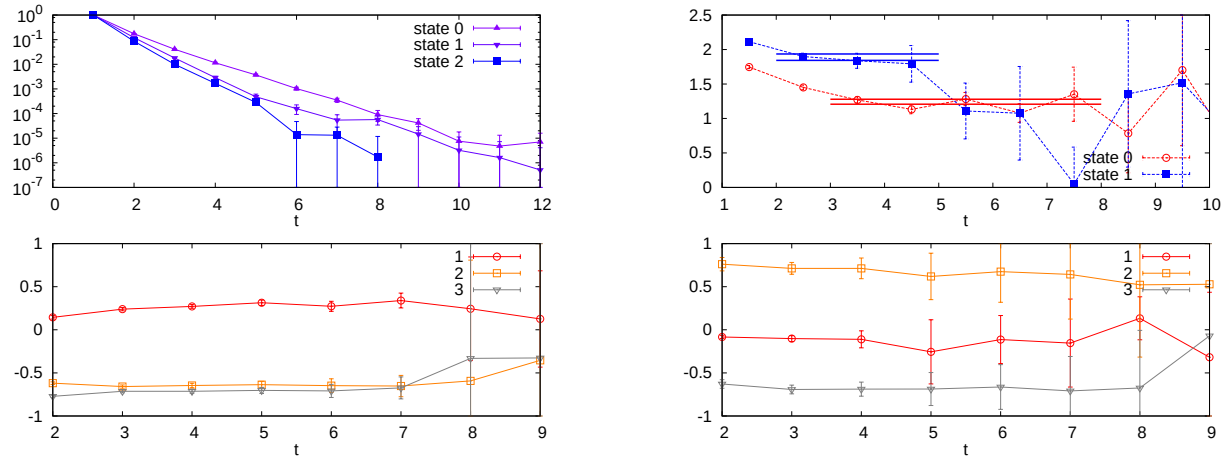

FIG. 11. $\Delta(-)$ with 16 eigenmodes subtracted: The correlators for all eigenstates (upper left), effective mass plot for the two lowest states (upper right), eigenvectors corresponding to the ground state (lower left). and 1st excited state (lower right).

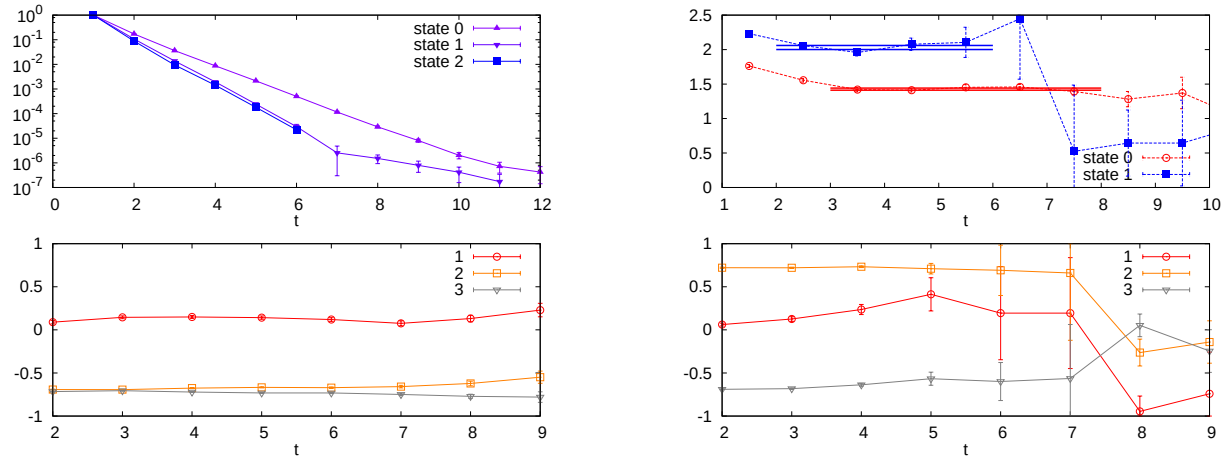

FIG. 12. $\Delta(-)$ with 128 eigenmodes subtracted: The correlators for all eigenstates (upper left), effective mass plot for the two lowest states (upper right), eigenvectors corresponding to the ground state (lower left). and 1st excited state (lower right).

breaking via the axial anomaly still persists. Then it follows that there is no direct interconnection of the lowest lying modes of the Dirac operator and the mechanism of the anomalous $U(1)_A$ breaking in QCD. Such a direct interconnection was suggested in the past through, e.g., the instanton fluctuations.

After unbreaking of the chiral symmetry the ρ and ρ' mesons become degenerate. What does this tell us? A degeneracy indicates some symmetry. The two distinct ρ states, ρ and ρ', lie in different irreducible parity-chiral representations, $(\frac{1}{2},\frac{1}{2})_a$ and $(0,1)+(1,0)$. In principle, their degeneracy could point out to a reducible representation of the parity-chiral group that would include both irreducible representations. Indeed, the product of two fundamental quark-antiquark chiral representations does contain, in particular, both $(\frac{1}{2},\frac{1}{2})_a$ and $(0,1)+(1,0)$:

$$[(0,\tfrac{1}{2})+(\tfrac{1}{2},0)]\times[(0,\tfrac{1}{2})+(\tfrac{1}{2},0)] \\ =(0,0)+(\tfrac{1}{2},\tfrac{1}{2})_a+(\tfrac{1}{2},\tfrac{1}{2})_b+(0,1)+(1,0)\,. \qquad (6)$$

Such a multiplet of dimension 16 (including isospin degeneracies) would consist of two distinct ω-mesons, f_1, h_1, two ρ-mesons as well as b_1 and a_1 mesons and would require a degeneracy of all of them. Now we do find, however, that the b_1 meson is well split from both ρ and ρ' after the unbreaking of the chiral symmetry. This rules out that the observed $\rho-\rho'$ degeneracy is related to restored chiral symmetry. The degenerate ρ and ρ' states are different because their eigenvectors are orthogonal and because they are well split before the removal of the low modes. This can be clearly seen from Figs. 13 and 14. This degeneracy indicates some higher symmetry that includes chiral $SU(2)_L\times SU(2)_R$ as a subgroup. It is a highly exciting question what this higher symmetry is. It will be seen from the following subsection that baryons also point to some higher symmetry.

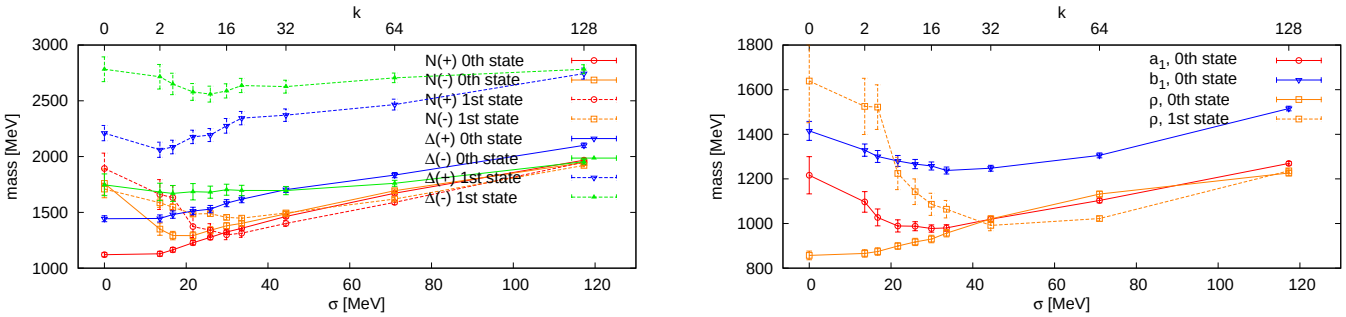

FIG. 13. Summary plots: Baryon (l.h.s.) and meson (r.h.s.) masses as a function of the truncation level.

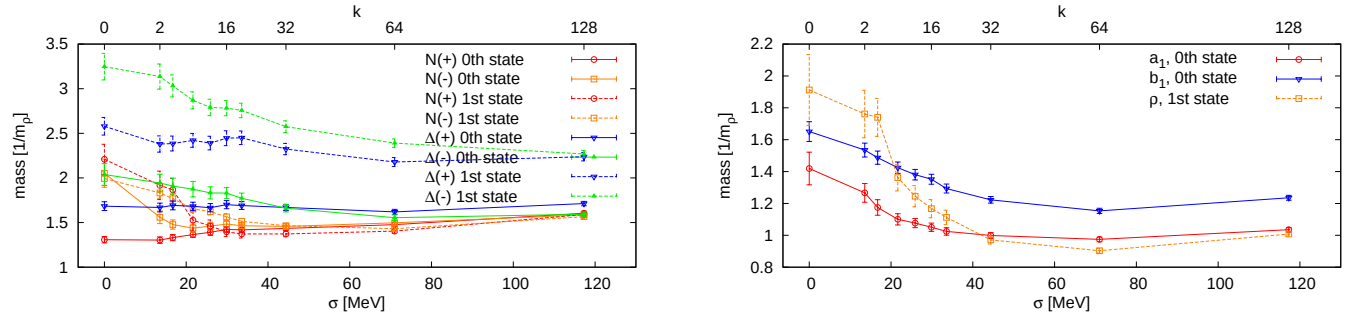

FIG. 14. Summary plots: Baryons (l.h.s.) and mesons (r.h.s.) in units of the ρ-mass at the corresponding truncation level.

D. Baryon chiral multiplets

If chiral symmetry is restored and baryons are still there they have to fall into (some of) the possible baryonic parity-chiral multiplets. There are three different irreducible representations of $SU(2)_L \times SU(2)_R \times C_i$ for baryons of any fixed spin:

$$(\tfrac{1}{2},0)+(0,\tfrac{1}{2})\,,\ (\tfrac{3}{2},0)+(0,\tfrac{3}{2})\,,\ (\tfrac{1}{2},1)+(1,\tfrac{1}{2})\,. \qquad (7)$$

The first representation combines nucleons of positive and negative parity into a parity doublet. The second representation consists of both positive and negative parity Δ's of the same spin. Finally, the third representation, that is a quartet, includes one nucleon and one Delta parity doublet with the same spin.

Extraction of the chiral eigenmodes of the Dirac operator leads to a systematic appearance of the parity doublets, as it is clearly seen from Figs. 13 and 14. There are two degenerate nucleon parity doublets with the same mass. There are also two distinct Δ parity doublets, but with different mass. Since our interpolators have spin $J=\frac{1}{2}$ for nucleons and $J=\frac{3}{2}$ for Delta's, we cannot see possible quartets of the $(\frac{1}{2},1)+(1,\frac{1}{2})$ type.

It is very interesting that the two nucleon parity doublets get degenerate, while the two Delta doublets are well split. The former hints at a higher symmetry for the $J=I=\frac{1}{2}$ states, while this higher symmetry is absent for the $J=I=\frac{3}{2}$ states.

E. On the origin of the hyperfine splitting in QCD

The $\Delta-N$ splitting is usually attributed to the hyperfine spin-spin interaction between valence quarks. The realistic candidates for this interaction are the spin-spin color-magnetic interaction [53, 54] and the flavor-spin interaction related to the spontaneous chiral symmetry breaking [55]. It is an old debated issue which one is really responsible for the hyperfine splittings in baryons. Our results suggest some answer to this question. Once chiral symmetry breaking is removed, which happens for the ground N and Δ states after extraction of the 50–60 lowest eigenmodes, the $\Delta-N$ splitting is reduced roughly by the factor 2. With the restored chiral symmetry the effective flavor-spin quark-quark interaction is impossible. The color-magnetic interaction is still there. This result suggests that in our real world the contribution of both these mechanisms to the $\Delta-N$ splitting is of equal importance.

VI. CONCLUSIONS

We have studied what happens with different mesons and baryons upon modifying the valence quark propagators by removing the lowest lying eigenmodes of the Dirac operator. These eigenmodes are directly related to the quark condensate of the vacuum via the Banks–Casher relation. Consequently, upon removal of the low-

est eigenmodes we artificially restore chiral symmetry, what we call "unbreaking" of the chiral symmetry. We study the evolution of the hadron masses with the number of extracted lowest eigenmodes in dynamical lattice simulations. There are a few interesting observations.

First, the quality of the signals from the hadrons after removal of the chiral eigenmodes of the valence quark propagators become much better than with the untruncated propagators. Most probably this is related to the fact that we artificially remove the pion cloud of the hadrons.

Second, from the spectral patterns both for the ground and excited mesons and baryons we conclude that confinement is still there while the chiral symmetry is artificially restored. Restoration of the chiral symmetry is evidenced by the fact that hadrons, both baryons and mesons, fall into different parity-chiral multiplets. At the same time there is a clear evidence that the broken $U(1)_A$ symmetry is not restored.

Third, some distinct parity doublets get degenerate upon chiral symmetry restoration. This indicates that there is some higher symmetry in the chirally restored regime, that includes the chiral group as a subgroup.

Finally, from the comparison of the hyperfine $\Delta - N$ splitting before and after unbreaking of the chiral symmetry we conclude that in our real world both the color-magnetic and the flavor-spin interactions between valence quarks are of equal importance.

ACKNOWLEDGMENTS

We would like to thank Georg P. Engel and Kim Splittorff for valuable discussions. The calculations have been performed on the SGI Altix 4700 of the LRZ Munich and on clusters at ZID at the University of Graz. Support by DFG SFB-TR55 and by the Austrian Science Fund (FWF) through grants P21970-N16 and DK W1203-N16 is gratefully acknowledged. M.S. is supported by the Research Executive Agency (REA) of the European Union under Grant Agreement PITN-GA-2009-238353 (ITN STRONGnet).

[1] L. Y. Glozman, Phys. Lett. B **475**, 329 (2000), arXiv:hep-ph/9908207.
[2] T. D. Cohen and L. Y. Glozman, Phys. Rev. D **65**, 016006 (2001), arXiv:hep-ph/0102206.
[3] T. D. Cohen and L. Y. Glozman, Int. J. Mod. Phys. **A17**, 1327 (2002), arXiv:hep-ph/0201242.
[4] L. Y. Glozman, Phys. Lett. B **539**, 257 (2002), arXiv:hep-ph/0205072 [hep-ph].
[5] L. Y. Glozman, Phys. Lett. B **587**, 69 (2004), arXiv:hep-ph/0312354.
[6] L. Y. Glozman, Phys. Rep. **444**, 1 (2007), hep-ph/0701081.
[7] R. L. Jaffe, D. Pirjol, and A. Scardicchio, Phys. Rev. D **74**, 057901 (2006).
[8] R. L. Jaffe, D. Pirjol, and A. Scardicchio, Phys. Rev. Lett. **96**, 121601 (2006), arXiv:hep-ph/0511081.
[9] R. L. Jaffe, D. Pirjol, and A. Scardicchio, Phys. Rept. **435**, 157 (2006), arXiv:hep-ph/0602010.
[10] M. Shifman and A. Vainshtein, Phys. Rev. D **77**, 034002 (2008), arXiv:0710.0863 [hep-ph].
[11] A. Anisovich, E. Klempt, V. Nikonov, A. Sarantsev, H. Schmieden, *et al.*, Phys. Lett. B **711**, 162 (2012), arXiv:1111.6151 [nucl-ex].
[12] T. A. DeGrand, Phys. Rev. D **69**, 074024 (2004), arXiv:hep-ph/0310303 [hep-ph].
[13] T. D. Cohen, Nucl.Phys. **A775**, 89 (2006), arXiv:hep-ph/0605206 [hep-ph].
[14] T. Schäfer and E. V. Shuryak, Rev. Mod. Phys. **70**, 323 (1998), hep-ph/9610451.
[15] T. A. DeGrand and A. Hasenfratz, Phys. Rev. D **64**, 034512 (2001), arXiv:hep-lat/0012021 [hep-lat].
[16] H. Neff, N. Eicker, T. Lippert, J. W. Negele, and K. Schilling, Phys.Rev. **D64**, 114509 (2001), arXiv:hep-lat/0106016 [hep-lat].
[17] T. DeGrand, Phys. Rev. D **64**, 094508 (2001), hep-lat/0106001 [hep-lat].
[18] T. DeGrand and S. Schaefer, Comput. Phys. Commun. **159**, 185 (2004), hep-lat/0401011.
[19] H. Neuberger, Phys. Lett. B **417**, 141 (1998), arXiv:hep-lat/9707022.
[20] H. Neuberger, Phys. Lett. B **427**, 353 (1998), arXiv:hep-lat/9801031.
[21] T. DeGrand and S. Schaefer, Nucl. Phys. (Proc. Suppl.) **140**, 296 (2005), hep-lat/0409056.
[22] L. Giusti, P. Hernández, M. Laine, P. Weisz, and H. Wittig, JHEP **04**, 013 (2004), hep-lat/0402002.
[23] G. S. Bali, S. Collins, and A. Schaefer, Comput. Phys. Commun. **181**, 1570 (2010), 0910.3970.
[24] G. Bali, L. Castagnini, and S. Collins, PoS **LATTICE2010**, 096 (2010), arXiv:1011.1353 [hep-lat].
[25] C. B. Lang and M. Schröck, Phys. Rev. D **84**, 087704 (2011), 1107.5195 [hep-lat].
[26] C. B. Lang and M. Schröck, PoS **LATTICE2011**, 111 (2011), arXiv:1110.6149 [hep-lat].
[27] M. Schröck, Phys. Lett. B **711**, 217 (2012), arXiv:1112.5107 [hep-lat].
[28] H. Suganuma, S. Gongyo, T. Iritani, and A. Yamamoto, PoS **QCD-TNT-II**, 044 (2011), arXiv:1112.1962 [hep-lat].
[29] S. Gongyo, T. Iritani, and H. Suganuma, "Gauge-invariant formalism with Dirac-mode expansion for confinement and chiral symmetry breaking," (2012), 1202.4130v1.
[30] G. E. Brown and M. Rho, Phys. Rev. Lett. **66**, 2720 (1991).
[31] L. Y. Glozman and R. F. Wagenbrunn, Phys. Rev. D **77**, 054027 (2008), arXiv:0709.3080 [hep-ph].
[32] L. Y. Glozman, Phys. Rev. D **79**, 037504 (2009), arXiv:0812.1101 [hep-ph].
[33] L. Y. Glozman, Phys. Rev. D **80**, 037701 (2009),

arXiv:0907.1473 [hep-ph].
[34] L. Y. Glozman, V. K. Sazonov, and R. F. Wagenbrunn, Phys. Rev. **84**, 095009 (2011), arXiv:1108.1681 [hep-ph].
[35] T. Banks and A. Casher, Nucl. Phys. B **169**, 103 (1980).
[36] J. C. Osborn and J. J. M. Verbaarschot, Phys. Rev. Lett. **81**, 268 (1998), hep-ph/9807490.
[37] M. Lüscher, JHEP **07**, 081 (2007), arXiv:0706.2298 [hep-lat].
[38] L. Giusti and M. Lüscher, JHEP **0903**, 013 (2009), arXiv:0812.3638 [hep-lat].
[39] S. Necco and A. Shindler, JHEP **04**, 031 (2011), arXiv:1101.1778 [hep-lat].
[40] K. Splittorff and J. J. M. Verbaarschot, Phys. Rev. D, **84**, 065031 (2011), arXiv:1105.6229 [hep-lat].
[41] C. Gattringer, Phys. Rev. D **63**, 114501 (2001), arXiv:hep-lat/0003005.
[42] C. Gattringer, I. Hip, and C. B. Lang, Nucl. Phys. B **597**, 451 (2001), arXiv:hep-lat/0007042.
[43] C. Gattringer, C. Hagen, C. B. Lang, M. Limmer, D. Mohler, and A. Schäfer, Phys. Rev. D **79**, 054501 (2009), arXiv:0812.1681 [hep-lat].
[44] G. P. Engel, C. B. Lang, M. Limmer, D. Mohler, and A. Schäfer, Phys. Rev. D **82**, 034505 (2010), arXiv:1005.1748 [hep-lat].
[45] S. Güsken *et al.*, Phys. Lett. B **227**, 266 (1989).
[46] C. Best, M. Göckeler, R. Horsley, E.-M. Ilgenfritz, H. Perlt, P. Rakow, A. Schäfer, G. Schierholz, A. Schiller, and S. Schramm, Phys. Rev. D **56**, 2743 (1997), arXiv:hep-lat/9703014.
[47] M. Lüscher and U. Wolff, Nucl. Phys. B **339**, 222 (1990).
[48] C. Michael, Nucl. Phys. B **259**, 58 (1985).
[49] T. Burch, C. Gattringer, L. Y. Glozman, R. Kleindl, C. B. Lang, and A. Schäfer, Phys. Rev. D **70**, 054502 (2004), arXiv:hep-lat/0405006.
[50] R. B. Lehoucq, D. C. Sorensen, and C. Yang, *ARPACK Users' Guide: Solution of large-scale eigenvalue problems with implicitly restarted Arnoldi methods* (SIAM, New York, 1998).
[51] C. Gattringer, L. Y. Glozman, C. B. Lang, D. Mohler, and S. Prelovsek, Phys. Rev. D **78**, 034501 (2008), arXiv:0802.2020 [hep-lat].
[52] G. P. Engel, C. B. Lang, M. Limmer, D. Mohler, and A. Schäfer, Phys. Rev. D **85**, 034508 (2012), arXiv:1112.1601 [hep-lat].
[53] A. De Rujula, H. Georgi, and S. L. Glashow, Phys. Rev. D **12**, 147 (1975).
[54] N. Isgur and G. Karl, Phys. Rev. D **18**, 4187 (1978).
[55] L. Y. Glozman and D. O. Riska, Phys. Rept. **268**, 263 (1996), arXiv:hep-ph/9505422.